12.7 AIRBORNE DUAL-DOPPLER RADAR OBSERVATIONS OF A BOW ECHO OVER MINNESOTA ON 3 JULY 2003 DURING BAMEX

David G. Lerach * and William R. Cotton
Colorado State University, Fort Collins, Colorado

1. Introduction

The relationship between bow-shaped convective systems and straight-line damaging surface winds has been noted on several accounts (e.g., Nolen 1959; Hamilton 1970; Fujita 1978). The prevailing hypothesis has been that the descending rear-inflow jet (RIJ), upon reaching the surface, was primarily responsible for the damaging winds (e.g., Burgess and Smull 1990; Weisman 1993; Pryzybylinski 1995). However, Schmidt and Cotton (1989) showed that a meso low at the apex of a derecho-producing squall line was associated with severe surface winds. Furthermore, extensive aerial and ground damage surveys of the aftermath of bow echoes have revealed small swaths of concentrated destruction not attributable to the RIJ (e.g., Forbes and Wakimoto 1983; Funk et al. 1999). Schmidt (1991), Bernardet and Cotton (1998), Weisman and Trapp (2003), and Trapp and Weisman (2003) performed numerical simulations of bow echo MCSs and found that the strong surface winds were induced by low-level mesovortices that formed on the leading edge of the bow echo just north of the apex. Weisman and Trapp (2003) and Trapp and Weisman (2003) found that the vortices were initiated at low levels through the tilting of initially crosswise baroclinic horizontal vorticity. These vortices induced a downward directed pressure gradient and a meso low that were responsible for the strong surface winds.

Atkins et al. (2005) combined a detailed damage survey with single-Doppler radar data and indeed found that numerous regions of straight-line surface wind damage were associated with low-level mesovortices that became tornadic. The authors noted that the tornadic mesovortices tended to be longer-lived and deepened and intensified rapidly prior to tornadogenesis compared to the nontornadic mesovortices, which tended to be weaker and shallower. Wakimoto et al. (2006a,b) verified the modeling results of Trapp and Weisman (2003) more thoroughly but found that the strongest surface winds were associated with the location where the RIJ flow and mesovortex rotation were in the same direction rather than local pressure gradients. More observational studies are needed to add robustness to these results.

The Bow echo And Mesoscale convective vortex (MCV) EXperiment (BAMEX) took place during the spring and summer of 2003, based out of Mid America Airport in Mascoutah, Illinois (Davis et al. 2004). The objective was to sample the multiscale aspects of bow echo and mesoscale convective MCSs. Utilizing both ground and airborne-based observing platforms, the field campaign observed 18 storm systems.

During the evening of 02 July 2003, a convective line developed in central Minnesota just southwest of a preexisting bow echo. The line was reinforced with 'back-building' cells and produced multiple bow echoes. A preliminary surface damage survey was constructed from NOAA storm report data (Fig. 1). It revealed a significant damage area associated with F0 winds, random regions with F1 damage, and a small pocket of F1 damage just north of the twin cities (arrow). This event took place within the time and spatial domain of BAMEX, and the Naval Research Laboratory (NRL) P-3 aircraft captured the evolution of the bowing MCS. This study discusses the synoptic and mesoscale environments in which the bow echoes formed and examines the mature stage of the convective line utilizing both ground-based and airborne dual-Doppler radar data. The goal of this study is to assess the kinematics and dynamics of the storm's primary mesovortices to further build our knowledge base regarding bow echo mesovortices and their connection with damaging surface winds.

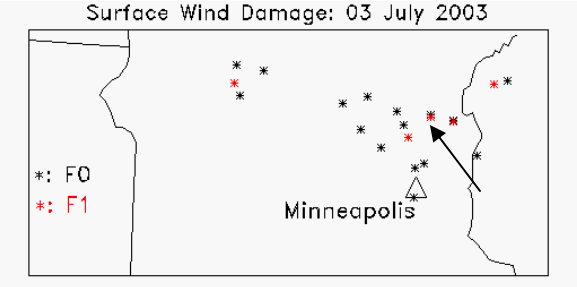

Figure 1: Severe wind reports from 3 July 2003. The arrow denotes F1 damage near the twin cities.

2. Environmental Conditions

The 300 hPa winds from 03 July 2003 0000 UTC (hereafter, all times UTC) revealed a ridge that extended northward into southern Manitoba and Ontario with weak jet streak patterns on either side (Fig. 2). The convective region of interest in central MN was situated under the ridge along its axis. While jet streak dynamics were an unlikely factor, the cut-off high-pressure circulation to the southwest and polar ridge to the north created a diffluence pattern in the winds over central MN with associated strong divergence, favoring lift over the area.

The 03 July 2003 500 hPa map at 0000 shows a subtropical high height (pressure) center over CO with its ridge extending northeast into northeastern MN, then back northwest into Ontario (Fig. 3). The

* Corresponding author address: David G. Lerach, Colorado State University, Dept. of Atmospheric Science, Fort Collins, CO 80523; email: dlerach@atmos.colostate.edu

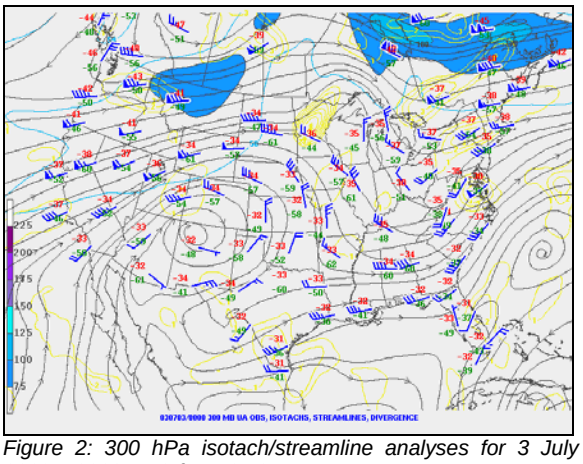

Figure 2: 300 hPa isotach/streamline analyses for 3 July 2003at 0000 UTC from SPC

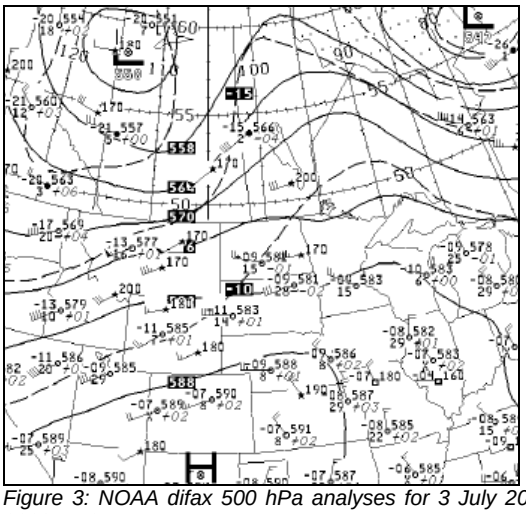

Figure 3: NOAA difax 500 hPa analyses for 3 July 2003 at 0000 UTC

reported winds at Bismark, ND and Aberdeen, SD along with the 5760 m and 5820 m height contours hinted at the presence of a short-wave trough over the focus region, extending south from northwestern MN through eastern SD. An Eta analysis of 500 hPa absolute vorticity for the same time indicated that a vorticity maximum was located just north of MN with a tongue of positive absolute vorticity that extended southward with the trough's axis (Fig. 4). The 0000 500 hPa analyses suggested that the convection was likely enhanced by positive vorticity advection associated with a mid-level short wave.

The short-wave trough is more clearly defined in the 700 hPa analyses for the same time period, extending northeastward from SD to northern MN (Fig. 5). Dew-point depression values indicate only moderate amounts of mid-level moisture present in the northern plains. Dew points at 700 hPa nearest to the convective area ranged from –3 to 1°C, corresponding to mixing ratios of roughly 5 g kg^{-1}. At 850 hPa for the same time, only weak warm air advection can be inferred in northwest MN (Fig. 6). However, dew-point depression values are smaller than those for 700 hPa and actual dew-points span 12

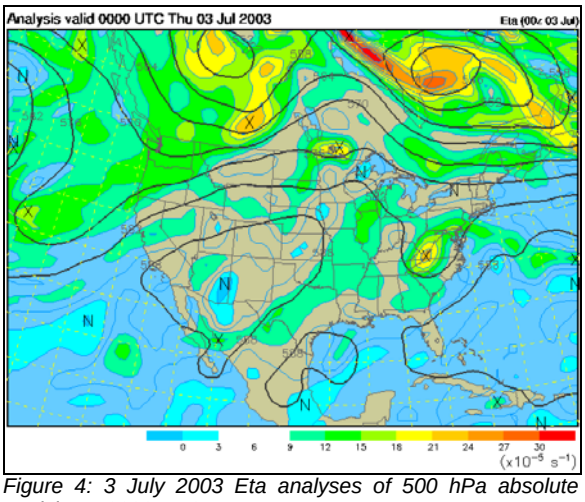

Figure 4: 3 July 2003 Eta analyses of 500 hPa absolute vorticity at 0000 UTC

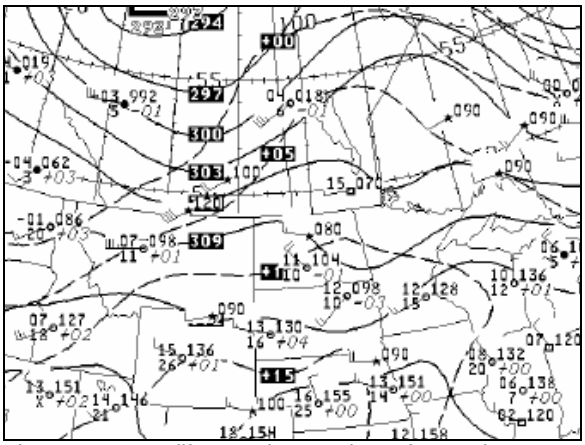

Figure 5: NOAA difax 700 hPa analyses for 3 July 2003 at 0000 UTC

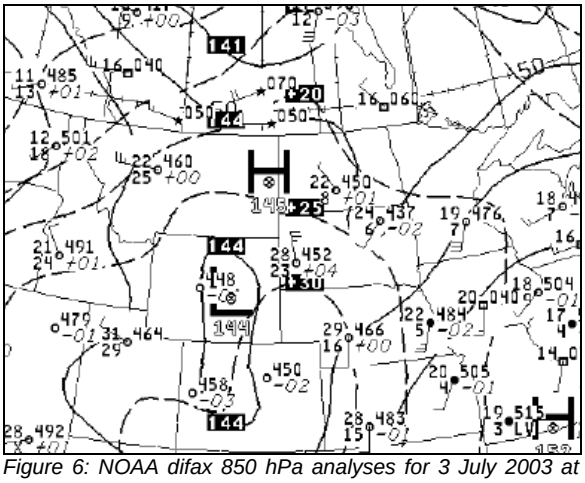

Figure 6: NOAA difax 850 hPa analyses for 3 July 2003 at 0000 UTC

to 18°C near the convective region, corresponding to mixing ratios greater than 10 g kg^{-1}. This suggests that there was a significant moisture presence at lower levels.

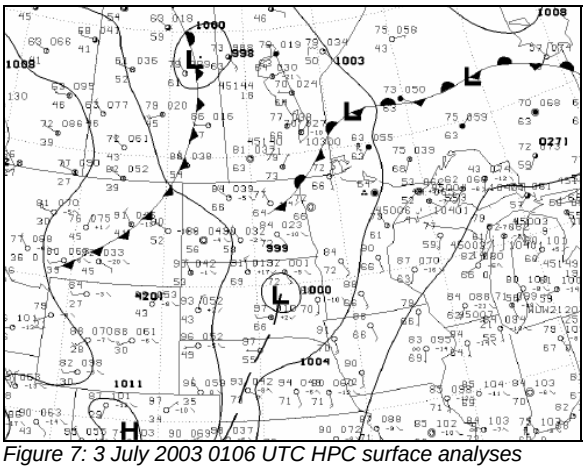

Figure 7: 3 July 2003 0106 UTC HPC surface analyses

Figure 7 displays the 3 July 2003 HPC surface analyses at 0106. A low-pressure center resided over eastern SD with a trough axis extending south towards the CO eastern border. Its circulation advected warm air (> 80°F) and high dew points (> 70°F) from the plains northward into southern and central MN. A stationary front was analyzed across eastern ND, northwestern MN, and into Canada: a placement similar to the location of the short-wave trough axis. Surface convergence together with both moisture and warm air advection at low levels strongly favored lift over MN at 0000. The 3 July 2003 0000 UTC synoptic pattern matched well with those from previous studies described to be favorable for bow echo development (Evans and Doswell 2000).

There was a large region of significant convective available potential energy (CAPE) between 1000 and 3000 J kg^{-1} that spanned central ND and SD through central MN by 3 July at 0000 (not shown). The 3 July 0000 sounding at Chanhassen, MN (Fig. 8) shows a nearly dry adiabatic temperature profile from the surface to 850 hPa while mixing ratios were greater than 10 g kg^{-1} below 850 hPa. Surface based CAPE was an estimated 1075 J kg^{-1} and the convective inhibition (CIN) was 235 J kg^{-1}. It should be noted that the Aberdeen, SD sounding for the same time exhibited similar conditions to Chanhassen but showed a CIN of only 12 J kg^{-1}. This suggested a strong potential for severe weather with little need for initial low-level forcing. The Chanhassen winds strongly veered from the surface to 550 hPa. The 0-5 km integrated shear was ~21 m s^{-1}. The sounding indicated the presence of conditional instability, significant CAPE, and low-level vertical wind shear that met the lower threshold for bow echo development (Coniglio et al. 2004).

3. Single Doppler radar analyses

Radar reflectivity images at 0.5° elevation angle from the KMPX WSR-88D on 3 July 2003 are shown in Fig. 9. The convective line of interest moved southeastward through central Minnesota with multiple rotation couplets evident in the velocity data (velocity data not shown). By 0357 (Fig. 9a) a cell

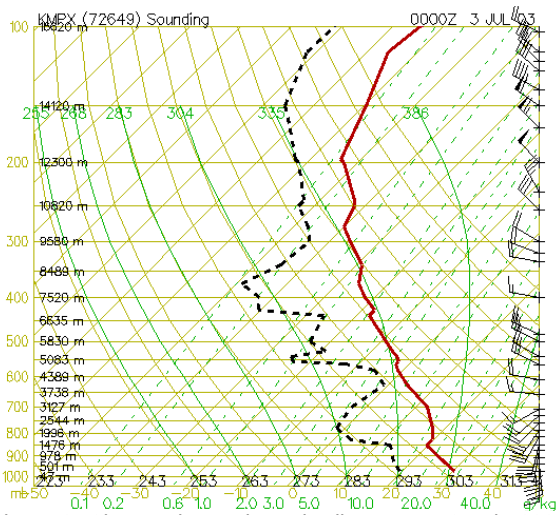

Figure 8: Skew-T thermodynamic diagram on 3 July 2003 0000 UTC for Chanhassen, MN (http://vortex.plymouth.edu)

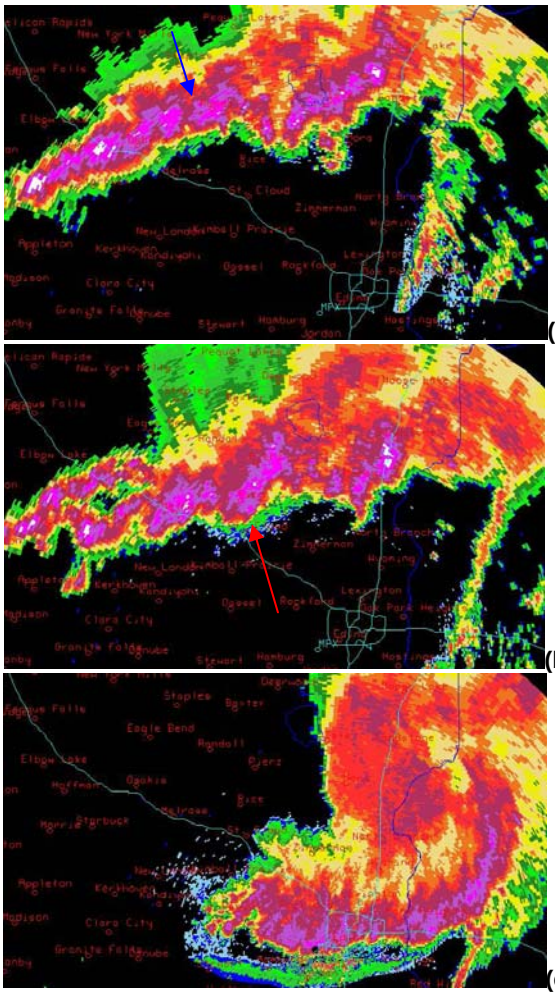

Figure 9: KMPX WSR-88D reflectivity factor for 3 July 2003 at (a) 0357 UTC (b) 0447 UTC and (c) 0701 UTC. The blue arrow (a) depicts the location and direction of the rear inflow. The red arrow (b) identifies the apex of the bowing segment.

exhibited strong rear inflow near 30 m s^{-1} just south of Eagle Bend, MN. This led to a bowing effect in the reflectivity signature and an apex near the rear inflow notch, as seen at 0447 (Fig. 9b). The Doppler velocities at this time suggested the presence of a low to mid level mesovortex immediately north of the bow apex, indicated by a strong cyclonic Doppler velocity couplet with an 'S'-shaped Doppler velocity boundary (Wakimoto et al. 2006b). By 0701 the convective line had entered its comma stage (Fujita 1978), seen as a bowing segment of reflectivity greater than 40 dBZ that stretched across southeastern Minnesota (Fig. 9c). By this time a gust front was apparent as a thin line of weak reflectivity that extended out ahead of the western half of the bow echo and along the apex.

4. Airborne Dual-Doppler radar analyses

The National Center for Atmospheric Research (NCAR) maintains and operates a 3-cm Electra Doppler radar (ELDORA) that flies aboard the NRL P-3, consisting of two antennas that use a variation of the fore-aft scanning technique (FAST) (Jorgensen et al. 1996). The NRL P-3 flew relatively straight paths at low levels along the convective line to resolve any small-scale mesovortices (Wakimoto et al. 2006a). The NRL P-3 flight path from 3 July is shown in Fig. 10. The ELDORA captured the majority of the convective system. However, the primary bow echo and associated mesovortices had begun formation before the radar began capturing their evolution. The NRL P-3 made three passes along the bowing segment. This section focuses on the mature and dissipating stages of the vortices. Note that the three dimensional, gridded, dual-Doppler datasets used in this study were created following the methods described in the appendices of Wakimoto et al. (2006a,b).

a. 04:56:28 – 05:05:05 UTC

Fig. 11 displays the ELDORA dual-Doppler wind syntheses at 400 m AGL for the flight leg 04:56:28 – 05:05:05. The bow apex is located in the lower left hand side of each figure, associated with an extensive rear inflow region where winds exceed 25 m s^{-1}. However, the winds are enhanced just northeast of the apex, exceeding 30 m s^{-1} and two pockets exist where the winds reach magnitudes of 35 m s^{-1}. Positive vertical air motions greater than 6 m s^{-1} exist all along the leading edge of the bow echo with a main updraft north of the apex exceeding 18 m s^{-1}. This updraft as well as those near the apex are accompanied by downdrafts on the order of 6 m s^{-1}, each located behind the leading edge. Two mesovortices are evident in the analysis seen as regions of positive relative vertical vorticity that exceed $12x10^{-3}$ s^{-1}. Both are positioned along the leading edge just north of the apex. The two maximum wind regions appear to be located to the southwest of the mesovortices where the RIJ flow and and vortex rotation are in the same direction. This is consistent with the findings of Wakimoto et al. (2006b). The southern vortex is located near a negative vorticity pocket of weaker intensity, located to the southeast. The southern mesovortex is associated with a slight hook in the reflectivity, and an 'S'-shaped pattern in the Doppler velocity gradient. The maximum vertical vorticity in these vortices do not reach $18x10^{-3}$ s^{-1}, meaning they are weaker than those found by Wakimoto et al. (2006a,b).

Fig. 12 shows a north-south cross-section through the primary mesovortex for the same time period. The location of the cross section is given as the distance between points A and A' in Fig. 11. It appears that the southern mesovortex extends to a height of 4 km while the northern vortex reaches 6 km. The northern vortex also reaches a maximum vorticity exceeding $18x10^{-3}$ s^{-1} near 4 km. The regions of maximum vorticity appear to be associated with Doppler velocity gradients (associated with the boundary between the RIJ and front-to-rear flow). The southern mesovortex compared best with the results of Wakimoto et al. (2006a,b). However, the northern mesovortex exhibited greater vertical extent and larger relative vertical vorticity at mid levels.

b. 05:05:56 – 05:17:14 UTC

Fig. 13 displays the ELDORA dual-Doppler wind syntheses at 400 m AGL for the flight leg 05:05:56 – 05:17:14. The maximum horizontal winds still lie north of the bow apex, however they no longer reach 35 m s^{-1}. The northern mesovortex still retains its shape to some degree. The southern vortex has lost its form and the positive relative vertical vorticity region now extends all along the leading edge of the convection with weaker negative vorticity pockets on either side. There is no longer a hook visible in the reflectivity and the 'S'-shaped Doppler velocity gradient signature is hardly visible. The vertical cross section through the leading edge of the system reveals that the once mesovortex is now a single column of weak positive relative vertical vorticity that extends through the upper levels of the storm system. There are relative vertical vorticity maxima near 4 km and near the surface with negative vorticity regions at low and mid levels behind the leading edge. The positive vorticity region tilts northward with height still following the Doppler velocity gradient near the boundary between the RIJ and upward front-to-rear flow.

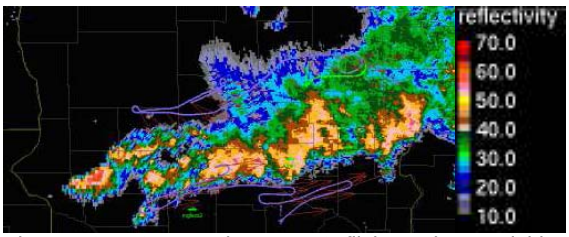

Figure 10: NOAA and NRL P-3 flight paths overlaid on composite reflectivity on 3 July 2003 (adapted from http://catalog.eol.ucar.edu/bamex/)

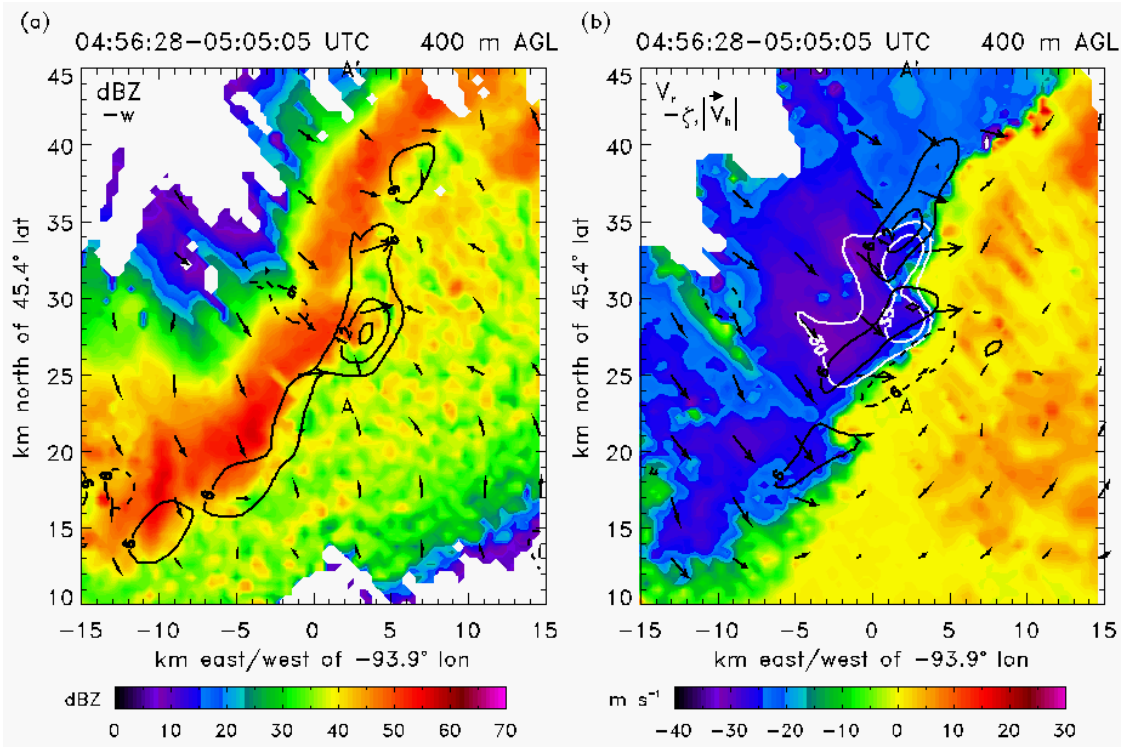

Figure 11: 0456-0505 UTC ELDORA Dual-doppler wind syntheses for 3 July 2003 of (a) color contoured reflectivity factor (dBZ) at 400 m AGL overlaid with storm-relative horizontal wind vectors and line contours of vertical velocity in m s^{-1} (solid positive, dashed negative) and (b) color contoured Doppler velocity at 400 m AGL overlaid with ground-relative horizontal wind vectors, black line contours of relative vertical vorticity (x10^{-3} s^{-1}) (solid positive, dashed negative), and horizontal winds with magnitudes greater than 30 m s^{-1} (white). Note that only reflectivity greater than 5 dBZ is shown in Fig. 11a.

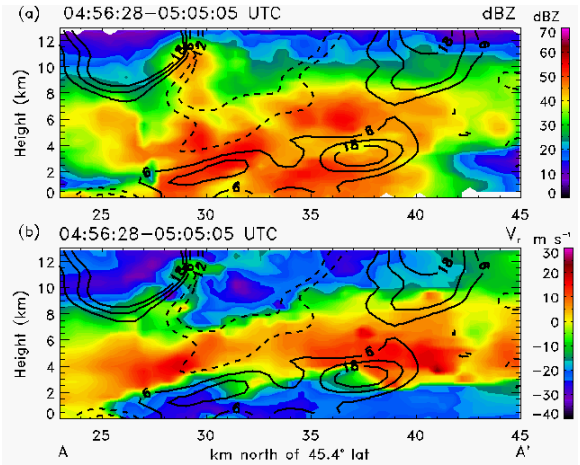

Figure 12: vertical cross section for 0456-0505 UTC color contouring (a) reflectivity factor (b) Doppler velocity. Relative vertical vorticity is line contoured in each figure (solid positive, dashed negative)

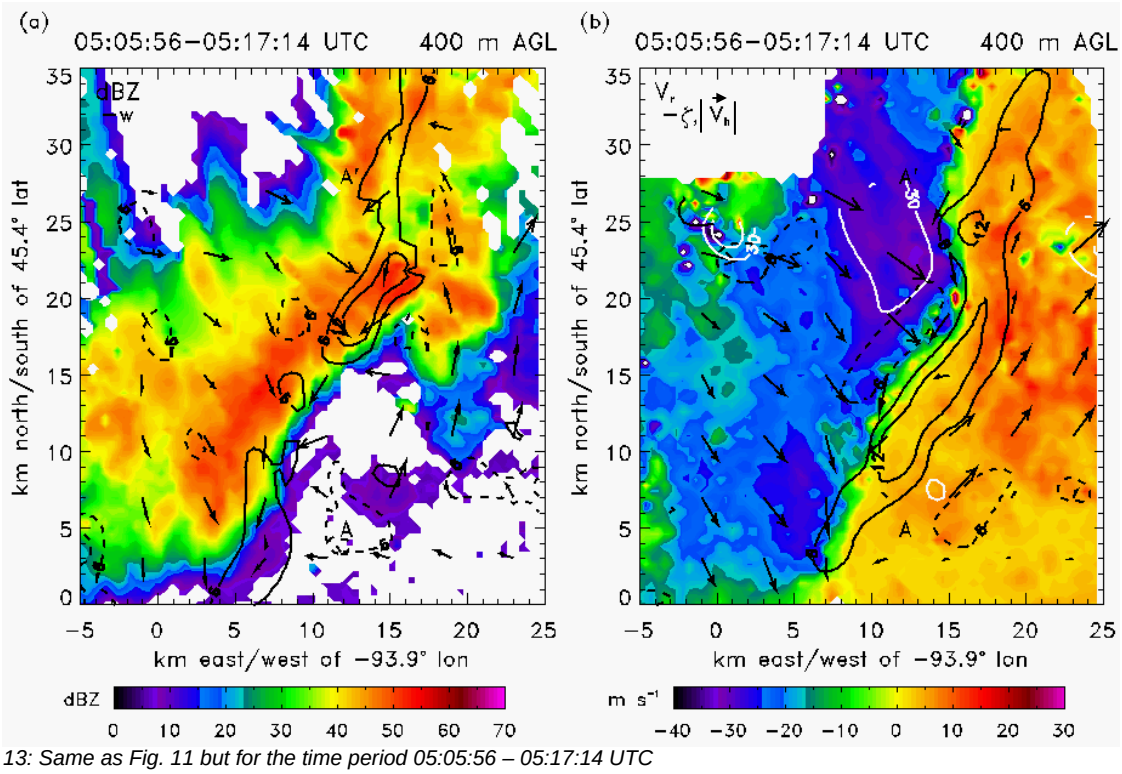

Figure 13: Same as Fig. 11 but for the time period 05:05:56 – 05:17:14 UTC

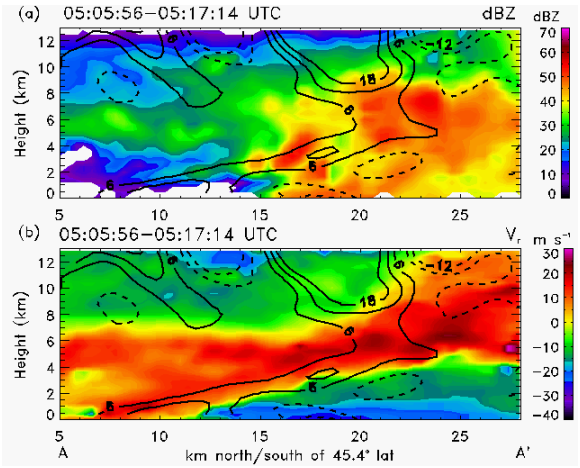

Figure 14: Same as Fig. 12 but for the time period 05:05:56 – 05:17:14 UTC

5. Backward trajectory analysis

Another alternative theory to that which states the RIJ being the source of strong surface winds in bow echo MCSs is based on simulations of derecho-producing squall lines by Schmidt (1991) and Bernardet and Cotton (1998). These studies showed that negatively buoyant air originating at low levels ahead of the squall line might account for a considerable portion of the severe winds behind the line. Air entering from ahead of the storm is lifted after encountering an upward-directed pressure gradient force, associated with an elevated region of low pressure formed by a rotating updraft or mesocyclone (perhaps mesovortex for this case). Once the stable air escapes this region of lift, it descends rapidly back towards the surface owing to the enhanced negative buoyancy from the melting and evaporation of precipitation. This “up-down” downdraft (Knupp 1987) is hypothesized to be an important driving force of bow echo MCSs and derechos. In this section, preliminary Lagrangian backward trajectory analyses are performed to identify possible source regions of downdraft air along and behind the 3 July leading convective line.

In the backward trajectory model utilized in this study, the three dimensional dual-Doppler dataset for a single flight leg was held constant in time. The location of a low level downdraft was tagged, and the eight surrounding grid points were tri-linearly weighted to calculate new trajectory u, v, and w wind components. The wind was multiplied by a designated time step (10 s in this study), which provided a new location. This process was repeated until the desired initial trajectory time was reached.

Backward trajectories were performed on the 04:56:28 – 05:05:05 flight leg when the low-level winds were at their strongest. Fig. 15 displays 300 m AGL downdrafts and storm-relative winds overlaid on background reflectivity factor at 600 m AGL. ‘x’ symbols denote 300 m AGL locations where backward trajectories were performed (located in contoured downdrafts). Black curves denote the ‘overhead view’ trajectory paths. Of the six trajectories shown, only the primary downdraft (‘D’) trajectory exhibits any front-to-rear motion. However, this motion appears to be associated with the location

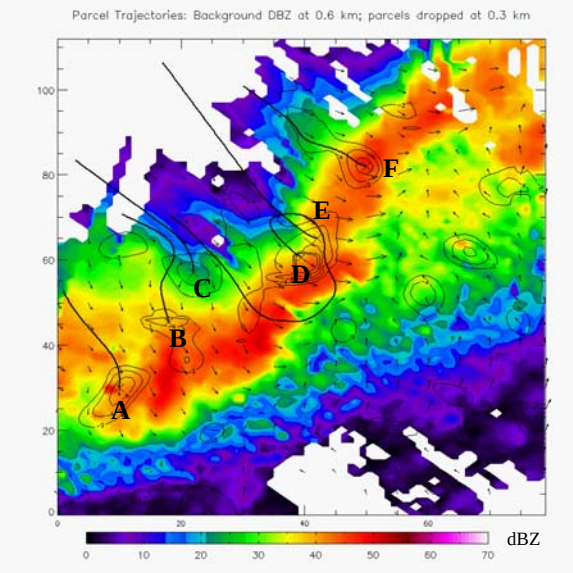

Figure 15: Back trajectories at 300 m AGL overlaid on color contoured reflectivity factor at 600 m AGL (dBZ), 300 m AGL downdrafts (contoured in m s^{-1}), and 300 m AGL storm-relative wind vectors

of the mesovortex (not shown) and the trajectory switches back to a 'rear-to-front' type movement.

This preliminary analysis reveals that the downdrafts primarily originated behind the convective line in the RIJ. The front-to-rear "up-down" downdraft was not present in this system at this time. It should be noted that these trajectory analyses were performed using a single flight leg. Some trajectories were calculated for over 30 min, while flight legs lasted approximately 10 min. New trajectories will be calculated based on multiple flight legs.

6. Summary and Discussion

During the evening of 3 July 2003, a severe convective line moved southeast through Minnesota producing multiple bow echoes and strong surface winds. Strong upper level divergence, a mid level short wave, and its associated positive absolute vorticity advection along with a moist, conditionally unstable environment and vertical wind shear created favorable atmospheric conditions for severe convection to occur.

The ELDORA dual-Doppler analyses indicated that the main bow echo was associated with a strong rear inflow jet and reflectivity notch at the bow apex. Mesovortices formed just northeast of the apex, the strongest associated with strong positive relative vertical vorticity, a hook in reflectivity, and an 'S'-shaped pattern in the Doppler velocity signature. The low level mesovortices coincided with significant positive vertical velocities and the strongest low level winds, where the flow of the RIJ and mesovortices were in the same direction. These observations compare well with the analyses of Wakimoto et al. (2006b). However, failure to capture the initial stages of mesovortex formation prevented verification that the vortices initially formed as relative vertical vorticity couplets. It is unclear at this time whether the mesovortices were connected with any regions of reported F1 damage at the surface. However, it is evident that the mesovortices found in this study were less severe than found by Wakimoto et al. (2006a,b) in an Omaha bow echo. The main mesovortex at peak intensity in this study was weaker and reached lesser vertical extent. These findings are consistent with the results of Atkins et al. (2005).

Preliminary backward trajectories were performed from 300 m AGL to determine the source region(s) of downdrafts that led to strong low-level winds. All of the downdrafts studied here were associated with descending rear-to-front flow. A more detailed trajectory study will be performed to verify this result.

Acknowledgments. The authors would like to thank Scott Loehrer of NCAR for assisting in raw ELDORA data acquisition, Lee Nelson of CSU for helping with WSR-88D visualization, and Paul Hein of CSU for assistance with CEDRIC data processing. Thanks go to Michael Bell of NCAR for assisting in ELDORA radar data quality control. Lastly, a special thanks to Hanne Murphey of UCLA for supplying the REODER and CEDRIC input code used to create the output three-dimensional dual-Doppler fields for this study. This work is supported by NSF, grant numbers ATM-0324234 and ATM-0638910.

References

Atkins, N. T., C. S. Bouchard, R. W. Przybylinski, R. J. Trapp, and G. Schmocker, 2005: Damaging surface wind mechanisms within the 10 June 2003 Saint Louis bow echo during BAMEX. *Mon. Wea. Rev.*, **133**, 2275-2296.

Bernardet, L. R., and W. R. Cotton, 1998: Multiscale evolution of a derecho-producing mesoscale convective system. *Mon. Wea. Rev.*, **126**, 2991-3015.

Burgess, D. W., and B. F. Smull, 1990: Doppler radar observations of a bow echo associated with a long-track severe windstorm. Preprints, *16th conf. On Severe Local Storms*, Kananaskis Park, AB, Canada, Amer. Meteor. Soc., 203-208

Davis, C., N. Atkins, D. Bartels, L. Bosart, M. Coniglio, G. Bryan, W. Cotton, D. Dowell, B. Jewett, R. Johns, D. Jorgensen, J. Knievel, K. Knupp, W.-C. Lee, G. McFarquhar, J. Moore, R. Przybylinski, R. Rauber, B. Smull, R. Trapp, S. Trier, R. Wakimoto, M. Weisman, and C. Ziegler, 2004: The Bow echo and MCV Experiment: Observations and opportunities. *Bull. Amer. Meteor. Soc.*, **85**, 1075–1093.

Coniglio, M. C., D. J. Stensrud, and M. B. Richman, 2004: An Observational Study of Derecho-Producing Convective Systems. *Weather and Forecasting*: **19**, 320–337.

Evans, J. S., and C. A. Doswell III, 2001: Examination

of derecho environments using proximity soundings. *Wea. and Forecasting,* **16**, 329-242.

Forbes, G. S., and R. M. Wakimoto, 1983: A concentrated outbreak of tornadoes, downbursts and microbursts, and implications regarding vortex classification. *Mon. Wea. Rev*., **111**, 220-235.

Fujita, T. T., 1978: Manual of downburst identification for project NIMROD. *SMRP Research Paper 156*, University of Chicago, 104 pp. [NTIS PB-28604801.]

Funk, T. W., K. E. Darmofal, J. D., Kirkpatrick, V. L. DeWald, R. W. Przybylinski, G. K. Schmocker, and Y.-J. Lin, 1999: Storm reflectivity and mesocyclone evolution associated with the 15 April 1994 squall line over Kentucky and southern Indiana. *Wea. Forecasting*, **14**, 976-993.

Hamilton, R. E., 1970: Use of detailed intensity radar data in mesoscale surface analysis of the 4 July 1969 storm in Ohio. Preprints, *14th Conf. on Radar Meteorology*, Tucson AZ, Amer. Meteor. Soc., 339-342.

Jorgensen, D. P., T. Matejka, and J. D. DuGranrut, 1996: Multi-beam techniques for deriving wind fields from airborne Doppler radars. *J. Meteor. Atmos. Phys*., **59**, 83-104.

Knupp, K. R., 1987: Downdrafts within high plains cumulonimbi. Part I: General kinematic structure. *J. Atmos. Sci*., **44**, 987-1008.

Nolen, R. H., 1959: A radar pattern associated with tornadoes. *Bull. Amer. Meteor. Soc*., **40**, 277-279.

Przybylinski, R. W., 1995: The bow echo: Observations, numerical simulations, and severe weather detection methods. *Wea. Forecasting*, **10**, 203-218.

Schmidt, J. M., 1991: Numerical and observational investigations of long-lived, MCS-induced, severe surface wind events: The derecho. Ph.D. dissertation, Colorado State university, Dept. of Atmospheric Science, Fort Collins, CO 80523, 196 pp.

Trapp, R.J., and M.L. Weisman, 2003: Low-level mesovortices within squall lines and bow echoes. Part II: Their genesis and implications. *Mon. Wea. Rev*., **131**, 2804-2823.

Wakimoto, R. M., H. V. Murphey, A. Nester, D. P. Jorgensen, and N. T. Atkins, 2006: High winds generated by bow echoes. Part I: Overview of the Omaha bow echo 5 July 2003 storm during BAMEX. *Mon. Wea. Rev*., **134**, 2793-2812.

__, H. V. Murphey, C. A. Davis, and N. T. Atkins. 2006: High winds generated by bow echoes. Part II: The relationship between the mesovortices and damaging straight-line winds. *Mon. Wea. Rev*., **134**, 2813-2829.

Weisman, M. L. 1993: The genesis of severe, long-lived bow echoes. *J. Atmos. Sci*., **50**, 645-670

__, and R. J. Trapp, 2003: Low-level mesovortices within squall lines and bow echoes. Part I: Overview and sensitivity to environmental vertical wind shear. *Mon. Wea. Rev*., **131**, 2779-2803.